New highly conductive nickel nanowire-filled P(VDF-TrFE) copolymer nanocomposites: elaboration and structural study

Antoine Lonjon, Lydia Laffont-Dantras, Philippe Demont, Eric Dantras, Colette Lacabanne

New Highly Conductive Nickel Nanowire-Filled P(VDF-TrFE) Copolymer Nanocomposites: Elaboration and Structural Study

Antoine Lonjon,[†] Lydia Laffont,[‡] Philippe Demont,*[,†] Eric Dantras,[†] and Colette Lacabanne[†]

Laboratoire de Physique des Polymères, CIRIMAT/Institut Carnot, Université Paul Sabatier, 118 route de Narbonne, 31062 Toulouse cedex 9, France, and CIRIMAT/Institut Carnot, ENSIACET, 118 route de Narbonne, 31077 Toulouse cedex 4, France

New highly electrical conductive nanocomposites were prepared by dispersing nickel nanowires into a poly(vinylidene difluoride)-trifluoroethylene P(VDF-TrFE) matrix. A suspension of individual nickel nanowires with a regular high aspect ratio ($\xi \approx 250$) was elaborated. The nickel nanowires were fabricated by electrodeposition using templates in anodic aluminum oxide with a nominal pore diameter of 200 nm, allowing a close control of nanowire crystallinity. Polycrystalline or single crystal nickel nanowires were obtained. An oxide layer was observed on nanowire surfaces after their extraction from the template. Physical and chemical treatments were used to completely remove the oxide layer. Scanning and high resolution transmission electron microscopy studies were performed. The elemental composition and the nature of the nanowires surface were investigated by electron diffraction and energy dispersive spectroscopy. Nickel nanowires without oxide layers were elaborated. The electrical conductivity of nanocomposite films was performed as a function of treated nickel nanowire volume fraction. A very low percolation threshold of 0.75 vol % was determined. Percolated nanocomposites filled by treated nanowires displayed a highly electrical conductivity value. The conductivity value obtained above the percolation threshold is the highest value known up to now in the case of a conductive nanoparticle dispersion.

Introduction

There is great interest for one-dimensional nanoparticles with high aspect ratio ξ ($\xi \approx 100-1000$) in nanocomposites elaboration. Nanomaterials such as carbon nanotubes (CNT),[1] nanorods,[2] and nanowires[3] enable the formation of high-performance nanocomposites[4−6] at a much lower concentration previously shown with standard microsized fillers. Metallic nanowires have attracted much attention because of their specific properties as mechanical resistance,[7,8] stiffness,[9] electrical conductivity,[10] and magnetic susceptibility.[11] These specific properties show that nanowires are excellent candidates to substitute the standard nanofillers in the formulation of multifunctional polymer nanocomposites.[12]

Several methods exist to synthesize metallic nanowires. One of them consists of growing a metallic germ in a solution by reducing metal ions. A growth direction is induced by using a capping agent. Silver nanowires have been obtained by this chemical method.[13] The other one uses the template technique as a support. Two ways are described in the literature: covering a high aspect ratio object by a metallic layer (positive template)[14] or filling a high aspect ratio support (negative template)[15] such as an anodic aluminum oxide (AAO) porous membrane.[16] This technique has been used for several years to produce metallic nanowires. The nanostructure shape depends on the template used. Template electrodeposition studies[17] have been focused on the maximal ratio obtained with the smallest nanometer pores.

One of the aims of this work is to synthesize metallic nanowires by the negative template technique without defects and so elaborate polymer nanocomposites having metallic behavior for electrical conductivity. The nanofiller volume fraction must be as low as possible to maintain the mechanical properties of the pristine polymer.

A great interest has been devoted to the chemical nature of the nanowire surface. In spite of their high specific chemical reactivity, the metallic behavior of the surface has to be promoted.

Experimental Methods

Nanowire Synthesis. Nickel nanowires (Ni NWs) were synthesized by electrochemical deposition in an anodic aluminum oxide (AAO) porous template. The electrolyte used for nickel deposition was a standard Watts bath with an accurate pH value of 4. Direct current (DC) electrodeposition was carried out at room temperature using a nickel wire as anode with 1.0 mm of diameter. A porous (AAO) membrane of 200 nm diameter and 50 μm thickness was supplied by Whatman. One side of the AAO membrane (silver back side) was coated with a 35 nm thickness silver layer by using a sputtering technique as cathode for electrodeposition. Nickel NW growth was controlled by the deposition time and the direct current intensity using a Keithley 2420 source meter. The AAO membrane was dissolved in NaOH 6 M for 30 min, releasing Ni NWs from the template. Then, Ni NWs were washed with distilled water and filtrated. A following sonication led to a very good dispersion of NWs in water or toluene.

An oxide layer was observed on Ni NWs which is responsible for the decrease of NW conductivity. Two methods were used to remove oxide layer. The first one was annealing under reducing atmosphere at 200 °C under H_2 atmosphere for 30 min. The second was dissolving of the oxide layer in a 0.25 M

Corresponding author. Telephone: +33561556538. Fax: +33561556221. E-mail: demont@cict.fr.
[†] CIRIMAT/Institut Carnot, Université Paul Sabatier.
[‡] CIRIMAT/Institut Carnot, ENSIACET.

solution of H_2SO_4 at 60 °C and stirring at 400 rpm for 5 min. The treated nanowires were filtered, rinsed with water, and stored in toluene or acetone. The same process was performed with H_3PO_4 acid as an alternative treatment.

Nanocomposite Preparation. Poly(vinylidene difluoride)-trifluoroethylene P(VDF-TrFE) 70/30 mol % copolymer was supplied by Piezotech S.A. (Saint Louis, France). The melting temperature was 150 °C determined by using a differential scanning calorimeter (Perkin-Elmer DSC7), and the density was about 1.8 g cm^{-3}. The nanocomposites were prepared by using a solvent casting method. P(VDF-TrFE) copolymer was dissolved in acetone. Treated Ni NWs were then poured into the polymer solution, and the mixture was submitted to a short pulse of sonication for 5 s, corresponding to a dissipated power of 25 W, to obtain a suitable dispersion of the nanowires in the polymer solution. A slight curvature of nanowires can be observed when a strong sonication is applied because of the metal nanowires' ductility and aspect ratio. The mild sonication used in this study allows nanowires to release from each other and their dispersion in the matrix, and does not affect the aspect ratio of nickel nanowires as seen in the different SEM images.

The solvent was evaporated using a magnetic stirrer at 80 °C for 1 h. Pellets of unaligned nickel nanowires randomly dispersed in P(VDF-TrFE) matrix were obtained. Films with a thickness of 200 μm were obtained using compression molding in a hot press at 200 °C under a pressure of about 0.3 MPa. No traces of solvent were observed during a thermogravimetric analysis (TGA) scan, indicating a complete removal of acetone.

Electron Microscopy. The morphology of the nickel nanowires was examined by scanning electron microscopy (SEM) using a JEOL JSM 6700F instrument equipped with a field emission gun (SEM-FEG). Nanocomposite samples were fractured at the liquid nitrogen temperature for observation by SEM. The structure and texture of the Ni NWs were determined by high-resolution transmission electron microscopy (HRTEM). A drop of the different NW suspensions was deposited on a copper grid coated with lacey carbon films to obtain transparent samples for electron irradiation. TEM and HRTEM images were obtained by using a FEI Tecnai F20 S-TWIN microscope. The elemental composition was also determined by energy dispersive spectroscopy (EDS) at a nanometre scale. The diffraction patterns were obtained using the selected area electron diffraction (SAED) mode.

Electrical Conductivity. Electrical conductivity measurements were carried out by recording the complex conductivity $\sigma^*(\omega)$ using a Novocontrol broadband spectrometer. The measurements were done in the frequency range from 10^{-2} to 10^6 Hz at room temperature. The real part, $\sigma'(\omega)$, of the complex conductivity $\sigma^*(\omega)$ was investigated. For all the nanocomposite samples considered in this study, the phase lag between the measured impedance and the applied ac voltage was negligible at low frequencies, so that the reported impedance at 0.01 Hz is equivalent to the dc resistance. The dc conductivity σ_{dc} of samples was determined from the independent frequency part of $\sigma'(\omega)$ (low frequency plateau). Films 200 μm thick were placed between two circular gold platted electrodes (20 mm in diameter). To reduce contact resistance with the cell electrodes, a thin layer of gold (100 nm) was sputtered onto both sides of the films using a BOC Edwards scancoat six SEM sputter coater.

Electrical Conductivity Percolation. The electrical performance of nanowire-filled polymer nanocomposites is strongly dependent on the volume fraction p and the aspect ratio (length to radius) L/r of the filler. In disordered systems, the insulator to conductor transition is driven by the percolation law where a critical volume fraction or percolation threshold of the filler is necessary for the onset of electrical conduction. According to the percolation theory, the dc conductivity σ_{dc} increases by a power law above the percolation threshold p_c:

$$\sigma = \sigma_0(p - p_c)^t \tag{1}$$

where σ_0 is a constant and t is the critical exponent.[18] For percolation in a lattice, t depends on the lattice dimension d: $t = 1.1-1.3$ for $d = 2$ and $t = 1.6-2$ for $d = 3$. The percolation threshold model in a three-dimensional sticks system, proposed by Balberg and Binenbaum,[19] shows that the percolation threshold is dependent on the aspect ratio and the anisotropy of sticks through their excluded volume V_{ex}. For that, the nanowires are capped cylinders with $L/r \gg 1$ and the associated excluded volume is defined as

$$V_{ex} = \frac{32}{3}\pi r^2 + 8\pi L r^2 + 4L^2 r\langle \sin\theta \rangle \tag{2}$$

where θ is the angle between two NWs and $\langle \sin\theta \rangle$ describes the degree of alignment of the NWs. For randomly oriented NWs, $\langle \sin\theta \rangle$ is equal to $\pi/4$ and eq 2 is written as

$$V_{ex} = \pi L^2 r = \frac{L}{r} V_{NW} \tag{3}$$

where V_{NW} is the NW volume. At the percolation threshold, V_{ex} is found to be constant. When NWs are randomly oriented, the critical excluded volume V_{ex}^{cr} is between 1.4 and 1.8 and is given by

$$V_{ex}^{cr} = \frac{L}{r} V_{NW} N_c = \frac{L}{r} f_c \tag{4}$$

where N_c and f_c are the NWs critical concentration and critical volume fraction for percolation, respectively.

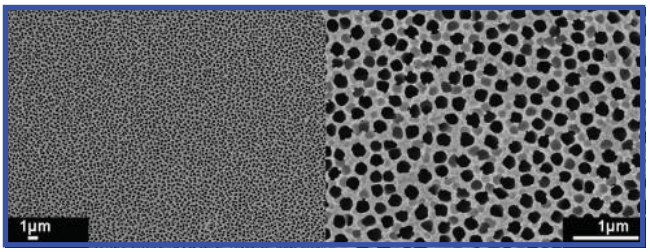

Figure 1. SEM images of the AAO membrane at two different magnifications before nickel electrodeposition.

Results and Discussion

Much interest has been devoted to the chemical nature of the nanowire surfaces. In spite of their high specific chemical reactivity, the metallic behavior of the surface has to be promoted.

The surface morphology of the AAO membrane was observed by SEM. Figure 1 shows an average pore diameter of about 200 nm with a very narrow distribution, and a pore density of about 5×10^8 pores cm^{-2} was estimated. The filling of the AAO membrane pores with nickel is performed by using direct current intensity ranging from 0 to 105 mA under a voltage of 3 V. The current density controls the deposition time. Ni NW growth

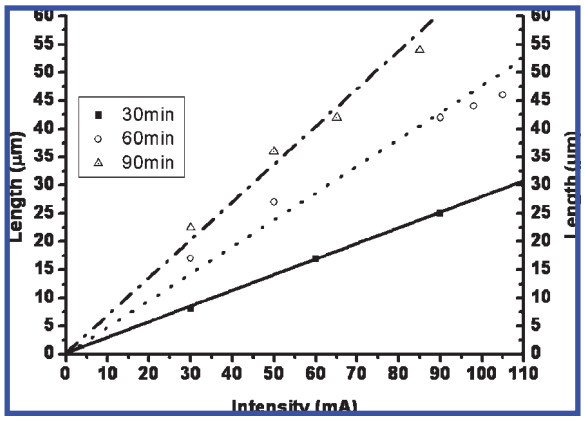

Figure 2. Nickel nanowire length as a function of the intensity of applied current for three electrodeposition times.

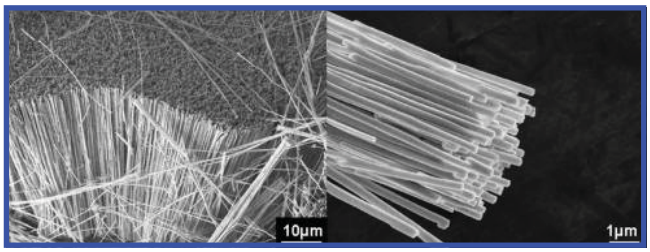

Figure 3. SEM image, at two magnifications, of nickel nanowires after complete removal of the AAO membrane but still anchored to the silver back side.

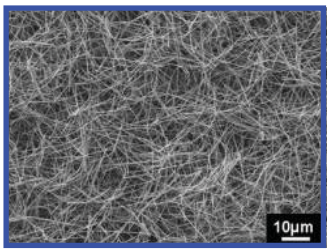

Figure 4. SEM image of nickel nanowires after complete removal of AAO membrane and silver back side and dispersion in acetone.

is dependent on the electron transfer which is regulated by the speed of the electron through the interface metal/solution and the kinetic transport of metallic ions to the electrode. Figure 2 shows the dependence of the time of deposition on intensity current. An extrapolation of the nanowire length L is also possible. A linear relation between the deposition time and the nanowire length is characteristic of behavior of charge transfer.

The nickel nanowire morphology was studied by SEM to determine the aspect ratio ξ. Figure 3 shows that Ni NWs are still attached to the silver coated layer backside of the alumina membrane, forming a "carpet fakir". NWs have a uniform length of 50 μm and a regular diameter of 200 nm. The silver coated layer backside and the AAO membrane were dissolved in HNO_3 and NaOH solution, respectively. Then the nanowire suspension was filtrated on 200 nm diameter polyamide membrane filter, and 12 mg of nickel nanowires per cm^{-2} was obtained. Nickel nanowires are well released from the membrane. Figure 4 shows the nickel nanowires releasing from the membrane. The density of Ni NWs is very high due to their suitable straightness. SEM confirms that Ni nanowire surfaces are smooth and continuous.

The conductivity of NWs is limited by two factors: the bulk resistivity and their contact resistance. The bulk resistivity is negligible compared to the contact one. An oxide layer formation occurs when the nanowires are released from the membrane

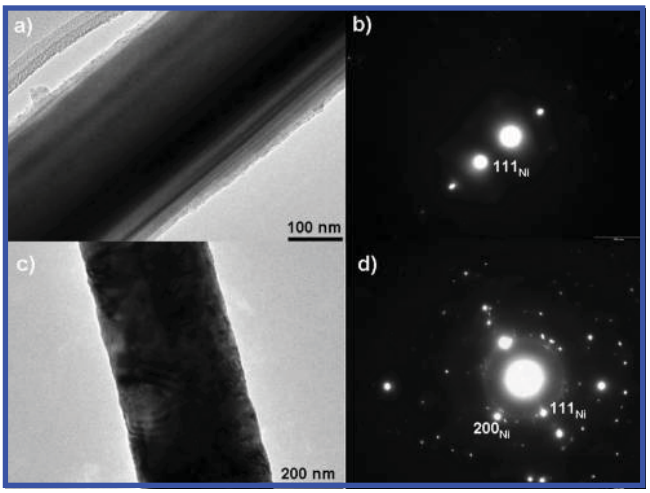

Figure 5. (a,c) Bright field TEM images of an individual nickel nanowire. SAED patterns (b) and (d) reveal, respectively, the single crystalline and polycrystalline nature of nickel.

and silver coated layer back side. The presence of the oxide layer is confirmed by conductivity measurements on pressed Ni NW samples for which a value of only 20 S m^{-1} is reached, a value drastically lower than that of nickel bulk: 1.56×10^7 S m^{-1}. The conductivity of Ni NWs treated with H_2SO_4 and H_3PO_4 acids is performed after rinsing with water then ethanol and dried at 50 °C for 30 min. NWs reduced with H_2SO_4 display a higher conductivity (115 S m^{-1}) than those reduced with H_3PO_4 (24 S m^{-1}).

Filtered nickel nanowires have been stored in acetone and dispersed using an ultrasonic bath. A droplet of this solution has been dried and deposited on an SEM pin. A good dispersion of the suspended nanowires without bundles is observed. The SEM image clearly shows that nickel nanowires are not damaged by sonication.

TEM images of a single nickel wire are shown in Figure 5a and c with their corresponding SAED patterns in Figure 5b and d. The average diameter is about 300 nm ((a) 330 nm; (c) 294 nm). The SAED pattern in Figure 5b shows single bright spots characteristic of nickel single crystals, while Figure 5d reveals polycrystallinity especially for the [111] direction, that is, the growth direction that is in good agreement with the literature.[20] Nevertheless, TEM characterizations of nickel nanowires have been performed in the literature,[17,20,21] but no results about the nature of the layer on the nanowire surfaces have been reported from the bright field TEM images. So the chemical nature and structure of the nanowires surface need to be well characterized.

The nickel nanowires, released after the silver backing and the alumina membrane dissolution, were examined by HRTEM. Figure 6 shows the bright field image of a nickel nanowire of 350 nm in diameter. One can see on the nanowire surface a discontinuous layer of varying thickness. Inset 1 in Figure 6 shows that the SAED pattern, taken from the end of the single nickel nanowire, confirms the nanowire to be Ni. The diffraction spots are well indexed to the face centered cubic (fcc) structure (JCPDS 65-2865). Inset 2 reveals both Ni and NiO phases. The NiO indexation has been done thanks to the JCPDS File (NiO: 75-0269; $Fm\bar{3}m$). The thin layer, visible only in the portion of the nanowire corresponding to SAED 2, confirms the surface of the NW to be oxidized. It is well-known that nickel oxidation can be limited by physical and chemical treatment.

The nickel nanowires, released after the silver backing and the membrane dissolution, were dispersed into water. Figure 7a shows a HRTEM image of a single nanowire of 270 nm in

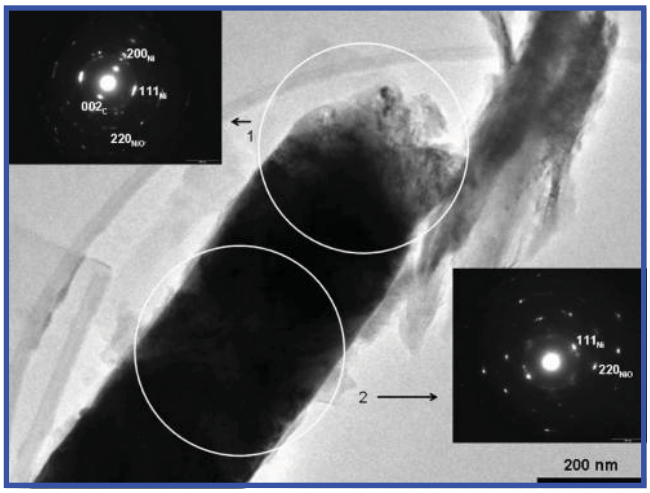

Figure 6. HRTEM image of the surface of an individual nickel nanowire and the SAED pattern taken from different portions of the individual wire.

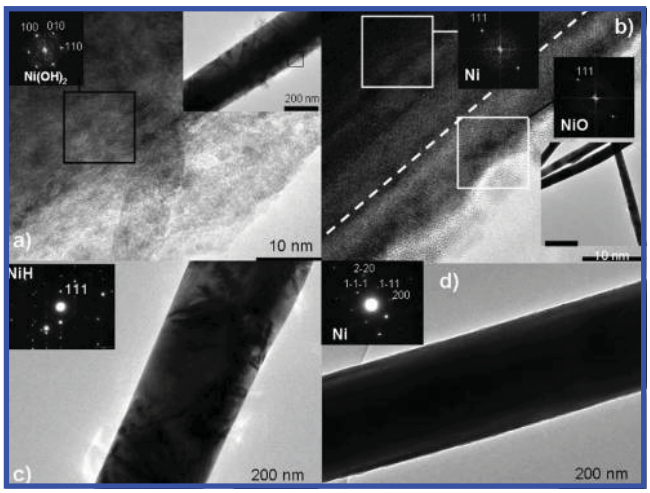

Figure 7. TEM and HRTEM images of individual nickel nanowire obtained after chemical treatments: (a) water, (b) sulfuric acid, (c) H_2 reduction, and (d) phosphoric acid. Insets in (a) an (b) show the two-dimensional Fourier transforms of the selected area at the surface of the nanowire. Insets in (c) and (d) show the corresponding SAED patterns.

diameter with some filaments on the surface. One part of the bright field image was acquired via high resolution, showing that the NW is covered by a Ni(II) hydroxylated oxide $Ni(OH)_2$ (JCPDS 03-0177, hexagonal) layer. To remove this oxide layer, the Ni nanowires are treated with sulfuric acid. The HRTEM image at low magnification (Figure 7b) shows that the surface of the nanowire is homogeneous and no filaments or layer are visible at this magnification. A high resolution image of one part of the NW is characteristic of a well-crystallized wire. The two-dimensional Fourier transform calculated from high resolution images of the inner and the surface of the nanowire shows diffraction spots representative of Ni and NiO phases. The passivation of nickel NW is topotactic because both phases have the [111] direction in common. A H_2 reduction has no effect on the nanowire surface as seen in Figure 7c (diameter of 241 nm). Nevertheless, the spacings in the SAED pattern

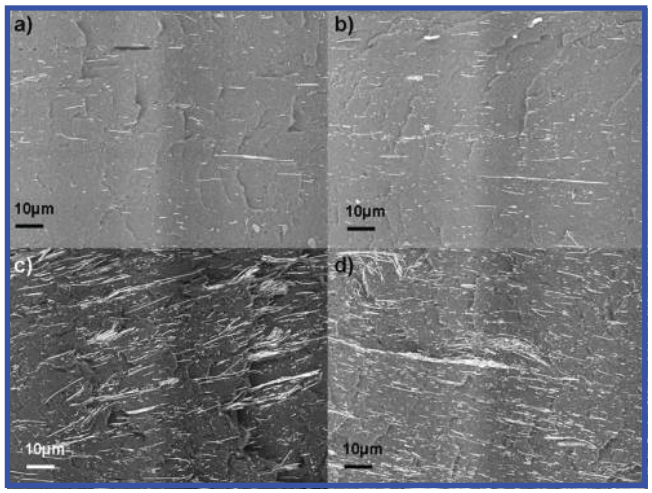

Figure 8. SEM images of the fracture surface of nickel nanowire/P(VDF-TrFE) copolymer composites at different Ni NW volume fractions: (a) 1 vol %, (b) 2 vol %, (c) 3 vol %, and (d) 4 vol %.

are in good agreement with spacings of the fcc NiH (JCPDS 65-0099). H_2 reduction has modified the chemical nature of the nanowires. Nickel nanowires have shown an ability to absorb hydrogen that confirms the Ni NWs as potential candidates for hydrogen storage.

The effect of phosphoric acid on NWs has also been investigated by TEM (Figure 7d). The aspect ratio of the NWs is not modified, and no oxide layer has been observed at high magnification. The corresponding SAED pattern of the bright field image is indexed by the fcc structure of the Ni phase, and the growth direction of the pure nickel nanowire is [200]. Sulfuric acid prevents massive oxidation and confers to nickel nanowires higher intrinsic electrical conductivity. Table 1 summarizes the chemical nature of the surface nanowire, observed by TEM, as a function of the chemical or physical treatment applied to nanowires.

Ni NW/P(VDF-TrFE) composites were prepared with a volume fraction of Ni NWs varying from 0 to 5 vol %. Figure 8 shows the SEM image of the polymer matrix filled by 1, 2, 3, and 4 vol % of Ni NWs. Nickel nanowires are clearly individual in acetone, and this homogeneous dispersion is conserved in P(VDF-TrFE) copolymer. The temperature and pressure conditions applied for the compression molding nanocomposite film processing involve a slight orientation of the nanowires.

The electrical conductivity of the insulating P(VDF-TrFE) copolymer is 10^{-12} S m^{-1} at room temperature. The dc electrical conductivity of the Ni NW/P(VDF-TrFE) samples at room temperature is plotted as a function of the NW volume fraction (Figure 9). The electrical conductivity increases drastically by 13 orders of magnitude at a very low percolation threshold of 1 vol % in comparison with the high value of 20 vol % observed for Ni spherical particles. The data are best-fitted by a scaling law according to eq 1 with $p_c = 0.75$ vol %, $\sigma_0 = 3.55 \times 10^{-3}$ S m^{-1}, and $t = 1.57 \pm 0.16$. The critical exponent value t is smaller than the universal value for three-dimensional percolation systems which is equal to 1.94. From the scaling law, σ_0 is an extrapolation at 100 vol % of NWs, which corresponds to the conductivity of Ni NW bundles. σ_0 is 5 orders of magnitude lower than the conductivity previously measured in Ni NWs.

TABLE 1: Chemical Nature of the Surface Nickel Nanowire as a Function of the Treatment

treatment	dispersion in H_2O	dispersion in C_7H_8	H_2 reduction	H_2SO_4 reduction	H_3PO_4 reduction
chemical nature of surface wire	$Ni(OH)_2$	NiO	NiH	NiO	Ni

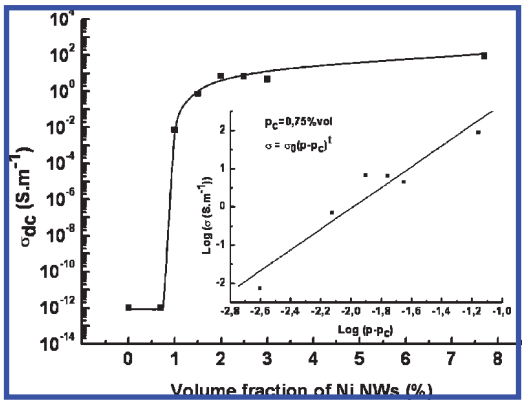

Figure 9. Dependence of the dc conductivity (σ_{dc}) on the nickel nanowire volume fraction in P(VDF-TrFE) matrix at 25 °C. The solid line connecting symbols is a guide for the eyes. The inset shows the log−log plot of σ_{dc} versus $(p - p_c)$ with $p_c = 0.75\%$ and $t = 1.57$. The solid line corresponds to the best-fitted line.

The Ni NWs display a narrow distribution of their aspect ratio around $\xi \approx 250$. Assuming the stick is Ni nanowire, we find a critical volume fraction of 0.64 ± 0.08 vol % according to eq 4, which is slightly lower than the experimental value of 0.75 vol %. This weak difference can be explained by the formation of a few poorly dispersed NW bundles. It is well-known that the percolation is dependent on the ability to disperse individually and uniformly the NWs in the polymer matrix. Such a low filler volume fraction is sufficient to establish a three-dimensional conducting network because of the high aspect ratio of Ni NWs. The measured conductivity arises from the electrical properties of nickel and the surface treatment of Ni NWs. A conductivity of 10^2 S m^{-1} is reached above p_c even if a value of only 10^{-1} S m^{-1} is measured on powder of spherical micrometer-sized nickel particles.[22] As a comparison, a conductivity value of about 1 S m^{-1} is obtained in Ni NWs without surface treatment.

Conclusion

We have successfully developed an easy method to produce a great quantity of nickel nanowires with controlled geometry, crystallinity, dispersion, and surface layer without oxide. Nickel nanowires with a high aspect ratio (∼250) were electrodeposited in an AAO template membrane. Elaboration of individual and uniformly dispersed nickel nanowires was reported. This electrodeposition method allows keeping the geometry of nanowires after the process and the dispersion in solvent. A quantity of 12 mg cm^{-2} of nickel nanowires was obtained in one time, suggesting an easy way to produce several grams. The electrodeposition parameters need to be adjusted in order to control the crystallinity of the Ni nanowires. The nanocomposite prepared by dispersing Ni NWs in P(VDF-TrFE) copolymer melt shows a very low percolation threshold: 0.75 vol %, preventing a damage of flexibility, weak density, and light weight of the copolymer matrix. An electrical conductivity of 10^2 S m^{-1} at such low filler content is the highest value to our knowledge. These results underline the key points and the essential parameters to elaborate highly conductive nanocomposites. The aspect ratio and the dispersion of nanofillers govern the percolation threshold, while the electrical conductivity of final conductive Ni NW/P(VDF-TrFE nanocomposites is supplied by the intrinsic conductivity of nickel nanowires. The composite conductivity value obtained slightly above the percolation threshold is the highest measured with high aspect ratio conductive nanomaterials.[23]

Acknowledgment. The work was supported by Direction Générale des Entreprises (DGE) and Conseil Région Midi-Pyrénées (CRMP) through NACOMAT contract.

References and Notes

(1) Iijima, S. *Nature.* **1991**, *354*, 56.
(2) Martin, C. R. *Chem. Mater.* **1996**, *8*, 1739.
(3) Penner, R. M.; Martin, C. R. *Anal. Chem.* **1987**, *59*, 2625.
(4) Barrau, S.; Demont, P.; Peigney, A.; Laurent, C.; Lacabanne, C. *Macromolecules* **2003**, *36*, 5187.
(5) Huynh, W. U.; Dittmer, J. J.; Teclemariam, N.; Milliron, D. J.; Alivisatos, A. P. *Phys. Rev. B* **2003**, *67*, 115326.
(6) Vivekchand, S. R. C.; Ramamurty, U; Rao, C. N. R. *Nanotechnology* **2006**, *17*, S344.
(7) Park, H. S.; Gall, K.; Zimmerman, J. A. *Phys. Rev. Lett.* **2005**, *95*, 255504.
(8) Wu, B.; Heidelberg, A.; Boland, J. J. *Nat. Mater.* **2005**, *4*, 525.
(9) Miura, S.; Kiguchi, M.; Murakoshi, K. *Surf. Sci.* **2007**, *601*, 287.
(10) Sun, Y. G.; Yin, Y. D.; Mayers, B. T.; Herricks, T.; Xia, Y. N. *Chem. Mater.* **2002**, *14*, 4736.
(11) Xu, J. X.; Huang, X. M.; Xie, G. Z.; Fang, Y. H.; Liu, D. Z. *Mater. Lett.* **2005**, *59*, 981.
(12) Park, J. M.; Sung-Ju, K. A.; Dong-Jin, Y. B.; Hansen, G.; Devries, K. L. *Compos. Sci. Technol.* **2007**, *67*, 2121.
(13) Sun, Y. G.; Gates, B.; Mayers, B.; Xia, Y. N. *Nano Lett.* **2002**, *2*, 165.
(14) Zhang, Y.; Dai, H. J. *Appl. Phys. Lett.* **2000**, *77*, 3015.
(15) Masuda, H.; Satoh, M. *Jpn. J. Appl. Phys.* **1996**, *35*, 126.
(16) Hulteen, J. C.; Martin, C. R. *J. Mater. Chem.* **1997**, *7*, 1075.
(17) Motoyama, M.; Fukunaka, Y.; Sakka, T.; Ogata, Y. H.; Kikuchi, S. *J. Electroanal. Chem.* **2005**, *584*, 84.
(18) Stauffer G. *Introduction to Percolation Theory*; Taylor & Francis: London, 1985.
(19) Balberg, I.; Binenbaum, N. *Phys. Rev. Lett.* **1984**, *52*, 1465.
(20) Wang, X. W.; Fei, G. T.; Xu, X. J.; Jin, Z.; Zhang, L. D. *J. Phys. Chem. B* **2005**, *109*, 24326.
(21) Pan, H.; Liu, B.; Yi, J.; Poh, C.; Lim, S.; Ding, J.; Feng, Y.; Huan, C.; Lin, J. *J. Phys. Chem. B* **2005**, *109*, 3094.
(22) Xu, H. P.; Dang, Z. M. *Chem. Phys. Lett.* **2007**, *438*, 196.
(23) Lin, B.; Gelves, G. A.; Haber, J. A.; Pötschke, P.; Sundararaj, U. *Macromol. Mater. Eng.* **2008**, *293*, 631.